An insight analysis of piston slap

Mohamed Riad Aly Ghazy
Faculty of Engineering, Zagazig University, Zagazig, Egypt

In this research, an analytical model is presented for the impact force and the vibratory response of the cylinder liner induced by the piston slap in internal combustion engines. In this model, the equation of motion for the coupled system of piston and cylinder liner is derived taking account of several modes of the cylinder liner to simulate accurately time histories of the impact force and the vibratory response. The piston slap phenomenon in a wet-liner, six-cylinder diesel engine is analyzed at different engine speeds using the dynamic characteristics of the cylinder liner, which are determined experimentally. The calculated results show that the impact force is amplified by the piston liner impact vibration. The calculated and measured vibrational time history and the frequency spectrum of the cylinder liner acceleration, are in good agreement.

تم في هذا البحث عرض أنموذج تحليلي للقوة الدفعية واهتزاز جدار الأسطوانة الناتج عن خبط المكبس في محركات الاحتراق الداخلي. وقد تم في هذا الأنموذج استنباط معادلة الحركة للنظام المكون من المكبس وجدار الأسطوانة مع الأخذ في الاعتبار أن جدار الأسطوانة له ترددات اهتزازية متعددة وذلك لكي يتم تمثيل التغير في قيمة قوي الخبط والاهتزاز الناتج مع الزمن بدقة. وتم تحليل ظاهرة خبط المكبس لمحرك ديزل ذي ستة اسطوانات ومبردّ بالماء عند سرعات دوران مختلفة للمحرك باستخدام الخواص الديناميكية لجدار الأسطوانة التي تم تعيينها بطرق معملية. وقد أظهرت النتائج أن قوي الخبط تزداد نتيجة اهتزاز جدار الأسطوانة ، وأن حسابات القوي العرضية المؤثرة علي المكبس وكذلك عجلة الاهتزاز لجدار الأسطوانة في تطابق جيد مع النتائج المقاسة معمليا.

Keywords : Piston slap, Liner vibration.

1. Introduction

In the internal combustion engines, piston slap causes engine noise [1] and liner cavitation [2]. It is an impact phenomenon between the piston and the cylinder liner when the side force acting on the reciprocating piston changes direction.

With a view to predicting noise and liner cavitation due to piston slap and reducing their levels, it is important to achieve an accurate estimate of the impact slapping force and the vibratory response of each engine part, e.g., liner.

Piston slap is a complex transient collision phenomenon [3, 4] on which the vibratory characteristics of the liner have a large influence. Many investigations of piston slap have been carried out both experimentally [5-7] and analytically (8-11]. The study of piston design and its motion has taken a great attention [12, 13]. The experimental investigations simulated to a great extent the gas presssure force, but the actual running conditions are different due to piston dynamics and its cross motion inside the cylinder. The analytical analysis always assumed gas presssure force as a unit step input.

In this study an analytical model of the piston slap, is presented taking into account the actual gas pressure force, impact force acting on the piston and the liner and the vibratory properties of the liner and engine block assembly.

2. Experimantal work

The studied engine is a six-cylinder, in-line dry-liner turbo-charges diesel engine. The bore and stroke are 116 and 129.5[mm], the piston and the connecting rod masses are 2.774 and 2.914[kg]. Its maximum speed is 2500[rpm].

The piston is freely hanged; using a robe, from its pin guide. An equipped B&K impact hammer type 8202 is used to apply the force and a B&K accelerometer type 4375 (2.6 gm)

is used for measuring the piston response. Both signals are fed to B&K charge amplifiers type 2635. The accelerometer signal is double integrated through the charge amplifier. The outputs of the charge amplifiers are acquired to a computer and used to calculate the receptance function (X/F) is then calculated (fig. 4).

The same procedure is repeated for the liner and the measured signals are used to calculate mobility function (V/F) for the liner (fig. 5).

The running engine is equipped with a pressure transducer B&K type 601-A. The measured signal is used to calculate the gas and piston side forces. The liner is equipped with accelerometers (B&K type 4375) fixed at the upper part (point "A" fig. 1) and at the lower part (point "B" fig. 1), to pick up the liner vibration at the appointed points when the engine is running.

3. Theoretical analysis

3.1. Definition of coordinate system and collision model

Referring to fig. 1, axis y is set at the center axis of the cylinder with upward positive direction. Axis x is taken at the TDC of the piston, passing through the center of the piston pin, while setting positive direction to the minor thrust side. Clockwise direction is set positive for the crankshaft rotational angle α and piston pin rotational angle θ_p.

It is assumed that the piston and the liner collide at the four points A, B, C, and D. The liner is treated as an elastic structure because there are several response points in the frequency range below 3kHz (fig. 5) in which the engine noise spectrum becomes dominant.

Fig. 4 shows that the piston first resonance frequency is higher than 3kHz. Therefore, in the frequency range below 3kHz, the piston can be treated as rigid body having a resilient spring at collision points.

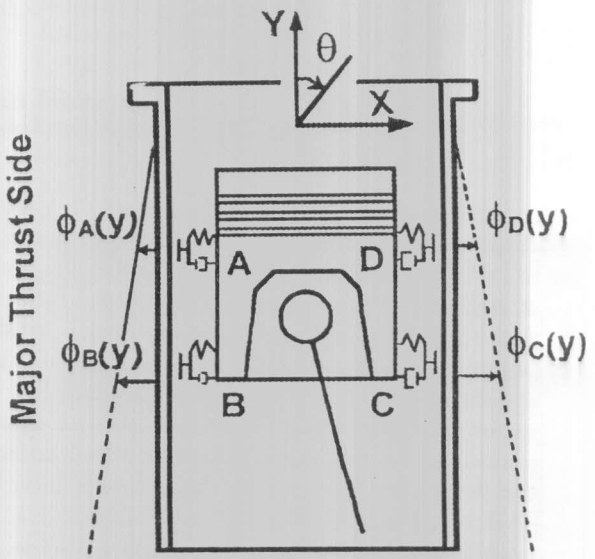

Fig. 1. Piston liner collision model and coordinate.

3.2. Forces acting on piston and liner

Forces acting between the piston and the liner are shown in fig. 2, where:

F_{IX} is the inertia force in transverse direction, due to piston motion

F_{IY} is the inertia force in vertical direction, due to piston motion

T_I is the rotational moment of inertia around the pin, due to piston tilt

F_g is the gas presssure force

F_t is the reaction force of connecting rod

T_p is the moment around the piston pin due to friction force between the piston and the piston pin

F_{rj} is the friction force in transverse direction between the j-th piston ring and the ring groove

F_{qj} is the friction force in vertical direction between the j-th piston ring and the liner

F_{f1}, F_{f2} are the friction forces in vertical direction between the piston and the liner

F_A, F_B, F_C, F_D are the impact forces between the piston and the liner

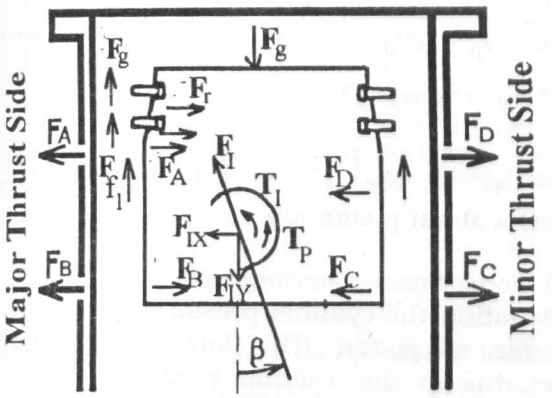

Fig. 2. Piston and liner system forces.

3.3. Inertia force and moment of inertia of piston

3.1.1. Piston and piston pin velocities

In fig. 3, the coordinates of the piston pin are represented by $P(x_p, y_p)$, its rotational angle by (θ_p), coordinates of the center of gravity of the piston by $G(x_G, y_G)$ and its rotational angle by (θ_G). The following relationship holds between the velocities at piston pin and the center of gravity of the piston and rotating angular velocities

$$\begin{aligned} \dot{x}_G &= \dot{x}_P + L_Y \dot{\theta}_P \\ \dot{y}_G &= \dot{y}_P - L_x \dot{\theta}_P \\ \dot{\theta}_G &= \dot{\theta}_P \end{aligned} \quad , \qquad (1)$$

where $\begin{vmatrix} L_\chi = \chi_G - \chi_p \\ L_Y = y_G - y_p \end{vmatrix}$.

3.3.2. Acceleration of piston in vertical direction

Assuming a constant rotating angular velocity (ω) for the crankshaft, vertical displacement (y_p) is uniquely defined by the rotational angle of the crank α. Referring to fig. 3, vertical acceleration of the piston pin $(\ddot{y}_p)$ when the piston pin offset (χ_{po}) is considered, is given approximately as follows;

$$\ddot{y}_p = -\gamma\omega^2 \left[\frac{\gamma^2 \ell^2 \cos^2(\omega t - \gamma_o) - A(\ell^2 - A^2)\sin(\omega t - \gamma_o)}{(\ell^2 - A^2)^{3/2}} + \cos(\omega t - \gamma_o) \right] \cdot \qquad (2)$$

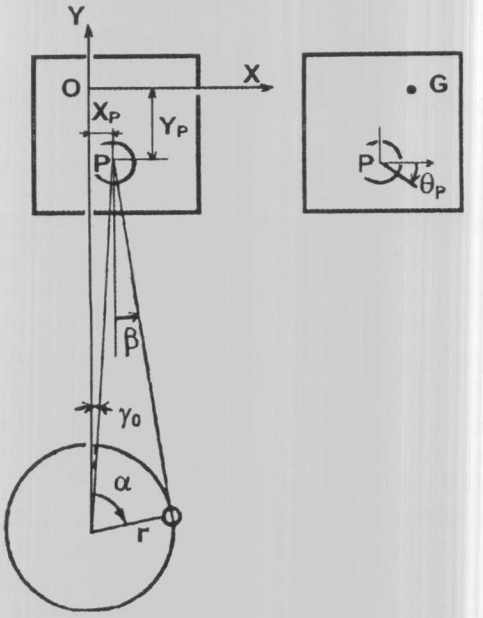

Fig. 3. Coordinate of the piston c.g and piston pin during motion.

Where;

ℓ is the connecting rod length,

r is the crank radius,

$$\sin\gamma_0 = -(\chi_p + \chi_{p0})/(\ell + r) \quad , \text{and}$$

$$A = \gamma \sin(\omega t - \gamma_0) - (\chi_p + \chi_{p0}).$$

3.3.3. Kinetic energy of piston (T)

From eq. (1), kinetic energy of the piston (T) is expressed as follows;

$$T = \frac{1}{2} m_p \left\{ \left(\dot{\chi}_p + L_y \dot{\theta}_p \right)^2 + \left(\dot{y}_p + L_\chi \dot{\theta}_p \right)^2 \right\} + \frac{1}{2} I_G \dot{\theta}_p{}^2 + \frac{1}{2} m_r \left(\dot{\chi}_p{}^2 + \dot{y}_p{}^2 \right) + \frac{1}{2} m_{rg} \dot{y}_p{}^2 . \quad (3)$$

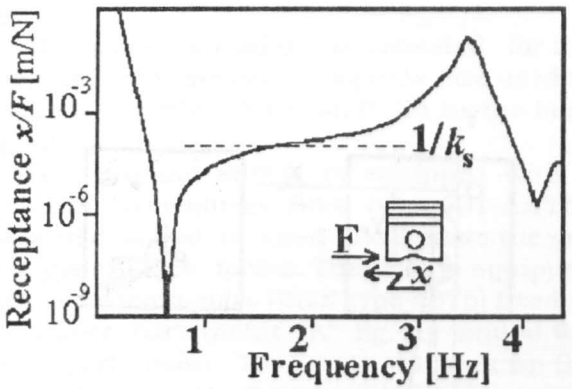

Fig. 4. Measured frequency response (receptance) of the piston.

Where;

m_p is the piston mass
m_r is the mass of piston pin and the small end of thr con. rod
m_{rg} is the piston ring mass
I_G is the piston moment of inertia.

3.3.4. *Inertia forces due to piston motion*

Transverse and vertical inertia forces at piston pin due to piston motion are represented by ($F_{I\chi}$) and ($F_{I\gamma}$,) respectively. Then eqs. (4, 5) are obtained from eq.(3) using Lagrange's eq. [9].

$$F_{I\chi} = \frac{d}{dt}\left(\frac{\partial T}{\partial \dot{\chi}_p} \right) - \frac{\partial T}{\partial x_p} = \left(m_p + m_r \right) \ddot{\chi}_p + m_p L_\gamma \ddot{\theta}_p , \quad (4)$$

$$F_{I\gamma} = \frac{d}{dt}\left(\frac{\partial T}{\partial \dot{y}_p} \right) - \frac{\partial T}{\partial y_p} = \left(m_p + m_{rg} + m_r \right) \ddot{y}_p - m_p L_x \ddot{\theta}_p . \quad (5)$$

Rotational moment of inertia about piston pin due to piston motion is given by

$$T_I = \frac{d}{dt}\left(\frac{\partial T}{\partial \dot{\theta}_p} \right) - \frac{\partial T}{\partial \theta_p} = I_p \ddot{\theta}_p + m_p L_\gamma \ddot{\chi}_p - m_p L_\chi \ddot{y}_p , \quad (6)$$

where $I_p = I_G + m_p \left(L_\chi{}^2 + L_y{}^2 \right)$ is the moment of inertia about piston pin.

3.3.5. *Force from connecting rod*

Denoting the cylinder pressure by (*p*), and diameter of piston (D), force acting onto piston due to the cylinder pressure is given by,

$$Fg = \frac{\pi}{4} D^2 * p . \quad (7)$$

Reaction force from the connecting rod (F_t) is determined by the equilibrium condition among vertical forces acting on the piston.

$$Ft = F_R - \frac{m_p L_\chi}{\cos\beta} \ddot{\theta}_p , \quad (8)$$

where

$$FR = \frac{\left(m_p + m_{rg} + m_r \right) \ddot{y}_p + F_g - \sum_{i=1}^{Nr} F_{qi} - F_{f1} - F_{f2}}{\cos\beta} .$$

The first term of eq. (8) is determined by the rotational angle of the crank while the second term is governed by the rotating motion of the piston.

3.3.6. Force and moment due to friction

Reaction force of the connecting rod (F_t)acts on the bearing of the piston pin. By representing the friction coefficient between the pin shaft and the pin bearing by (μ_p,) moment around the pin (T_p) is expressed by

$$T_p = \mathrm{sgn}(\dot{\phi}) \mu_p R_p F_t , \quad (9)$$

where,

R_p is the piston pin radius,

$$\dot{\phi} = \dot{\beta} - \dot{\theta}_p \text{ , and } \quad sgn(\dot{\phi}) = \begin{cases} 1 ..... & \dot{\phi} > 0 \\ -1 ..... & \dot{\phi} < 0 \end{cases}.$$

Vertical friction force between j-th piston ring and the liner is given by the following equation using friction coefficient between the ring and the liner (μ_{qj})

$$F_{qj} = -sgn(\dot{y}_p)\mu_{qj} W_j \pi D \text{ ,} \qquad (10)$$

where W_j represents compressive load per unit length of the j-th ring which is calculated by the method shown in [4].

Transverse friction force between the j-th piston ring and the ring groove (F_{rj}) is given by eq. (11) using friction coefficient (μ_{rj}).

$$F_{rj} = -sgn(\dot{\chi}_{rj})\mu_{rj} F_{qj} \text{ ,} \qquad (11)$$

where $\dot{\chi}_{rj}$ represents the transverse velocity of the pin at the position of the j-th ring.

Vertical friction force between the piston and the liner (F_{f1}), (F_{f2}) using friction coefficient (μ_f) are expressed as follows;

$$F_{f1} = sgn(\dot{y}_p)\mu_f (F_A + F_B) \text{ ,}$$

$$F_{f2} = -sgn(\dot{y}_p)\mu_f (F_C + F_D), \qquad (12)$$

where F_A to F_D are impact forces between the piston and the liner.

3.3.7. *Impact force between piston and liner*

Impact force F_S between the piston and the liner at collision point (S), is given by eq.(13) using spring constant (K_s) and damping coefficient (C_s), that simulate the dynamic stiffness of the piston and the damping effect of the oil film.

$$F_s = -\delta_s \{K_s(\chi_{ps} - \chi_{Ls}) + C_s(\dot{\chi}_{ps} - \dot{\chi}_{Ls}) \text{ , (13)}$$

where δ_s = 1 colliding
= 0 not colliding

As shown in fig. 4, spring constant (K_s), at the collision point of the piston is estimated by using the measured results of the driving receptance at the collision point of the piston. The constant becomes 400MN/m at the upper part of the piston skirt and 250MN/m at its lower part.

Since the formation of oil film in the actual engine has not been examined completely under operating condition, damping coefficient can not be determined theoretically, consequently, the damping coefficient is estimated.

4. Vibration response of piston and liner system

4.1. Equation of motion for piston system

The piston is regarded as a rigid body having a resilient spring at the collision point with the liner. In addition, vertical motion of the piston pin is uniquely determined by the rotational angle of the crank. Therefore, transverse displacement (χ_p) at piston pin position, and rotating angle (θ_p) around the piston pin, are considered. The equation of motion for the piston is given by the following equation according to the equilibrium of forces acting on the position as mentioned above.

$$\begin{bmatrix} m_p + m_r & m_p(L_y - L_\chi \tan\beta) \\ m_p L_\gamma & I_p \end{bmatrix} \begin{bmatrix} \ddot{\chi}_p \\ \ddot{\theta}_p \end{bmatrix} = \begin{bmatrix} f_\chi \\ f_\theta \end{bmatrix}, \qquad (14)$$

where;

$$f_\chi = F_t \sin\beta + \sum_{r=1}^{Nr} F_{rj} + \sum_{S}^{A-D} F_S \text{ ,} \qquad (15)$$

$$f_\theta = m_p L_\chi \ddot{y}_p - F_g(\chi_t - \chi_p) - \sum_{j=1}^{2} F_{fj}(\chi_{fj} - \chi_p) - T_p + \sum_{r=1}^{Nr} F_{rj}(y_{rj} - y_p) + \sum_{S}^{A-D} F_S(y_S - y_p) \text{ , (16)}$$

N_r is the number of rings.

χ_t is the x coordinate of the upper center of piston

χ_{fj} is the x coordinate at piston where friction force between the piston and the liner is acting.

y_{rj} is the y coordinate of the j-th ring.

4.2. equation of motion of liner system discrete expression of equation of motion

As the liner and engine block are considered as an assembly, the effect of the engine block must be taken into account when evaluating the vibratory response of the liner. In this paper, a combined system of engine block and liner is referred to as "the Liner system".

The equation of motion for the liner system, where impact force with piston f is acting, is expressed as follows by using mass matrix M, damping matrix C and stiffness matrix K, for the liner system.

$$M\ddot{u} + C\dot{u} + Ku = f \ . \qquad (17)$$

Where u represents the displacement vector of liner system.

4.3. *Dynamic characteristics of liner system*

The dynamic characteristics of liner system, including engine block, can be obtained by either calculation or vibration test. fig. 5 shows the measured result of the driving point mobility for the liner of a wet liner engine. From the result of such a vibration test, the modal parameters of the liner system (natural circular frequency (ω_n), normal mode (ϕ_n), effective mass ($\tilde{m}_n$), effective damping ration (ζ_n), suffixes n represent the relevant quantity relates to the n-th mode) can be identified by using curve fit technique shown in [14]. Where the influence of damping is negligible, the following orthogonality holds with mass matrix M and stiffness matrix K [15].

$$\Phi^t M \Phi = \begin{bmatrix} \ddots & & \\ & \tilde{m}_n & \\ & & \ddots \end{bmatrix} , \quad \Phi^t K \Phi = \begin{bmatrix} \ddots & & \\ & \tilde{m}_n \omega_n^2 & \\ & & \ddots \end{bmatrix} . \qquad (18)$$

Where $\Phi = (\Phi_1, \ldots, \Phi_N)$ is the matrix of vibration mode. In addition the following orthogonality is assumed also for the damping matrix C.

$$\Phi^t C \Phi = \begin{bmatrix} \ddots & & \\ & 2\zeta_n \omega_n \tilde{m}_n & \\ & & \ddots \end{bmatrix} . \qquad (19)$$

4.4. Vibratory response of liner system

Vibratory displacement u of the liner system, impacted by the piston, is represented by a linear combination of the normal modes ϕ_n from the first to N^{th} mode, as follows ;

$$u = \Phi_1 a_1 + \ldots + \Phi_N a_N = \sum_{n=1}^{N} \Phi_n a_n \ , \qquad (20)$$

where a_n is the modal response of the n^{th} mode.

Substituting into the equation of motion for liner system , eq. [17), taking into account the orthogonality previously mentioned, eqs. [18, 19), the equation of motion for the n-th mode is represented as following;

$$\ddot{a}_n + 2\zeta_n \omega_n \dot{a}_n + \omega_n^2 a_n = \sum_{S}^{A-D} \phi_n(y_S) F_S / \tilde{m}_n \ . \qquad (21)$$

In the above equation, the n-th normal mode ϕ_n (y_s) at impact point S changes dependent on the rotational position of the crank.

4.5. *Piston - liner system vibration response*

The piston and the liner are subjected to coupled vibration via impact force F. The equations of motions for the piston and the liner, namely eq. (14) and eq (21), are reduced to simultaneous ordinary differential equations. Thus, the vibratory responses of the liner and the piston can be obtained at each crank angle, together with the time histories of impact force.

5. Example of calculation

5.1. Test condition:

Table 1 shows the test conditions. The dynamic characteristics; shown in fig. 5, of the liner system including engine block are obtained from the result of a vibration test. Clearance between the piston and the liner is calculated using measured temperature of the piston [1] and liner vibration measurements [16].

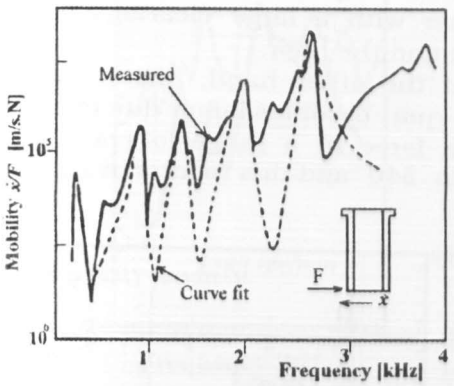

Fig. 5. Measured frequency response (mobility) of the liner.

5.2. Gas, inertia and piston side forces

Fig. 6 shows gas, inertia and piston side forces at 1800 and 2300 rpm. The cylinder pressure changes approximately 3% depending on rotational speed. However, the inertia force changes about 40%. Accordingly, the side piston force near the top dead center becomes larger at 1800 rpm. However, away from TDC, the side force at 2300 rpm becomes larger.

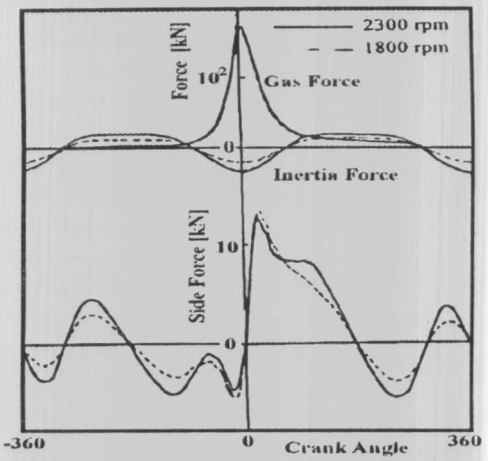

Fig. 6. Piston side force at different engine speeds

5.3. Impact force, and its spectrum

Fig. 7 shows the time history of impact force between the upper and lower parts of the piston in the vicinity of the TDC. In this case, the piston, being pressed to the minor thrust side before, starts to move toward the major thrust side when the sign of the piston side force changes, and collides with the liner. At the upper part of the piston, the greater relative clearance to the liner results in an increased impact velocity. Furthermore, because of large spring constant of the upper part of the piston, an impulsive force is generated at the point of impact.

Table 1
Test conditions of calculation

Cycle	4	
Bore x Stroke	135 x150 mm	
Load	full load	
Impact Points	y_U =30 , y_L =-65 mm	
Impact Stiffness	K_U =400 , K_L =25 MN/m	
Impact Damping	C_U = C_L = 10KN/m/s	
Engine Speed	1800	2300
$P_{max.}$	11.6	12 MPa
Piston -Liner Clearance	δ_U = 20 μm	δ_U = 10 μm
	δ_L = 85 μm	δ_L = 55 μm

suffix U : Upper , L : Lower

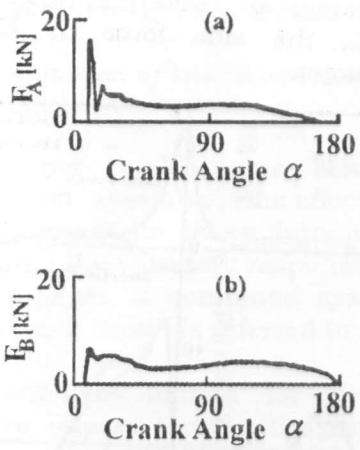

Fig. 7. Piston impact force upper and lower (b) parts of the piston.

Fig. 8 shows the frequency spectra of the piston side force and the impact force at the upper and lower parts of the piston. Components below 500Hz consist mainly of piston side force, however in the frequency range between 1 and 3 kHz, it can be seen that the components introduced by the transient impact of the piston slap are dominating the spectrum.

5.4. Liner vibration and its spectrum:

When measuring the spectra of gas pressure, vibration signals, ... etc, the important issue is to determine the peak values and the corresponding frequencies (fig. 5). It is sometimes the custom to draw the spectrum envelope for comparison reasons. The valley values carry no importance at all.

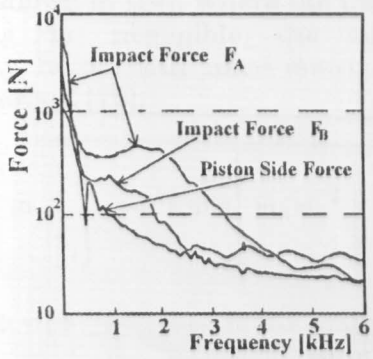

Fig. 8. Spectra of forces acting on the piston.

Fig. 9 compares calculated and measured vibratory acceleration at lower part of the liner at 1800 and 2300 rpm. fig. 10 shows a comparison between calculated and measured spectra of vibrating acceleration for the liner.

Calculated values substantially agree with measured ones in time domain, maximum values and frequency spectra, of acceleration response of liner.

The acceleration response at 1800 rpm is larger than in 2300 rpm in the vicinity of the TDC. This is because piston side force becomes larger in the vicinity of the TDC together with a large clearance between the piston and the liner.

On the other hand, piston side force at 2300 rpm becomes larger due to influence of inertia force in a range of crank angle from 360 to 540 and this results in greater piston slap.

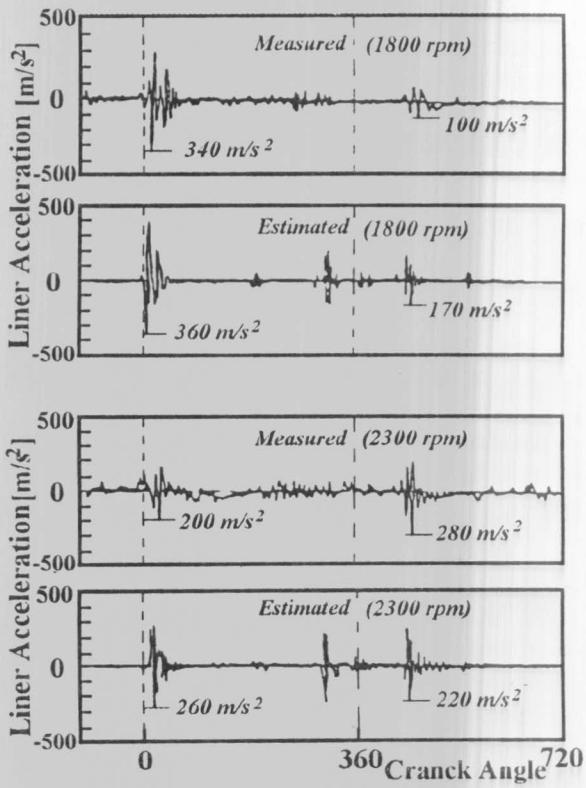

Fig. 9. Measured and estimated liner vibration acceleration (time domain).

In the frequency range higher than 3kHz, calculated liner acceleration spectrum (fig.10) is smaller than measured values. This is because the dynamic characteristics of the liner are taken into account only up to 2.7 kHz. Moreover, calculated spectrum becomes smaller at frequencies lower than 1.5 kHz, because liner vibration lower than 1.5 kHz is more strongly affected by vibration of engine block which is subjected to other exciting forces such as bearing impact force.

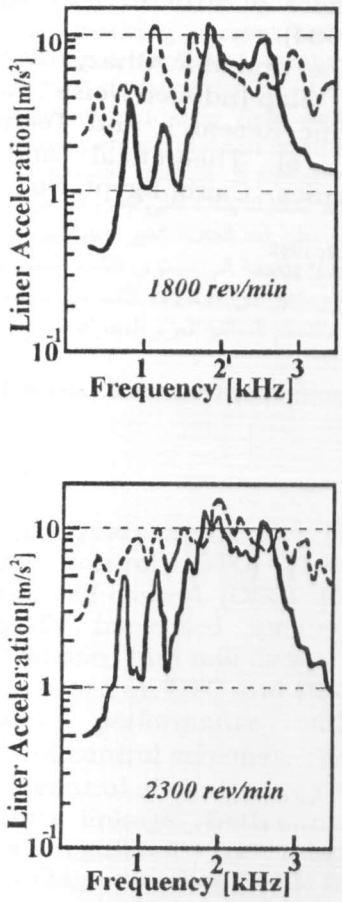

Fig. 10. Measured (dotted) and estimated (solid) liner vibration acceleration (frequency doain).

6. Conclusions

This paper describes a method of simulation calculation for piston slap phenomena, one of the major causes of engine noise and liner vibration and cavitation. The accuracy of the method is confirmed by experiment.

This method enables the analysis of coupled impact vibration between the liner and the piston. According to this method, the dynamic characteristics of a liner coupled to an engine block are taken into account. A spring and dashpot are assumed at the impact point for simulating the dynamic stiffness of the piston and damping of oil film. Finally, the impact condition is analyzed by time step integration technique.

Impact force and the vibratory response of the liner, as obtained by the proposed method, will be applicable to estimating engine noise and liner cavitiation.

A calculation for simulation is performed using the measured dynamic characteristics of a liner of an actual engine in the condition of full load and two engine speeds namely; 1800, 2300 rev/min.

Calculated time history and frequency spectra of liner acceleration substantially agreed with measured results, verifying the effectiveness of the proposed calculation method and its application to the study of reducing piston slap.

References

[1] T. Priede, "In Search of Origins of Engine Noise- An Historical Review", SAE Paper 800534 (1980).

[2] A.S.H. Lowe, "Analytical Technique for Assessing Cylinder Liner Cavitation Erosion", SAE Trans. Vol. 99, pp. 439-448 (1990).

[3] K.C. Vora and B. Ghosh, "Vibration Due to Piston Slap and Combustion in Gasoline and Diesel Engines", SAE Preprints No. 244, pp. 167-177 (1991).

[4] Y.C. Zhou, "Working Conditions of the Piston in the Cylinder Diagnosed by Engine Surface Vibration", Neiranji Gongcheng, Vol. 6 (3), pp. 54-60 (1985).

[5] R.G. Dejong and N.E. Parsons, "High Frequency Vibration Transmission Through The Moving Parts of An Engine" SAE Paper 800405 (1980).

[6] A. Miura, "Piston Slap", Nissan Diesel Giho, No. 45, (1982).

[7] M.D. Rohrle, "Affecting Diesel Engine Noise by Piston". SAE Paper 750799 (1975).

[8] K. Tsuda, and T. Koizumi, "Mechanics of Piston Slap", JSME Transaction, Vol.. 40 (334) (1974).

[9] E.E. Ungar and D. Ross, "Vibration and Noise Due to Piston Slap in Reciprocating Machinary", J. Sound and Vibration, Vol. 22, pp. 547-575 (1965)

[10] S.S. Haddad and D.A. Howard, "Analysis of Piston Slap Induced Noise and Assessment of Some Method of Control in Diesel Engines", SAE Paper 800517 (1980).

[11] T. Yonezawa, H. Kanida and K. Katsuragi, "Study on Cavitation Erosion of the Cylinder liner", JSME Trans., C. Vol. 50 (459) (1984).

[12] Sam-D. Haddad and Tjan Kektjen, "Analytical Study of Offset Piston and Crankshaft Designs and The Effect of Oil Film on Piston Slap Excitation in a Diesel Engine", Mechanism & Machine Theory, Vol. 30 (2), pp. 271-284 (1995).

[13] S.D. Haddad, "Theretical Treatment of Piston Motion in I.C.Engines for the Prediction of Piston Slap Excitation", Mechanism and Machine Theory, Vol. 30 (2), pp. 253-269 (1995).

[14] I. Honda and Y. Irie, "A Method of Modal Parameter Estimation from Measured Frequency Response", ASME, Structural Dynamics, PVP, Vol. 98-6 (1985).

[15] W.C. Hurty and M.F. Rubin`stein, "Dynamics of Structures", Prentice-Hall, Inc. (1984).

[16] E.H. Gad and M.R. Ghazy, "In Search of Piston Slap Induced Noise", Academy of Scientific Research and Technology 3rd Conf. of Theoretical and Applied Mechanics, Cairo, Egypt, Nov. (1988).

Recived September 1998
Accepted January 1, 2000